Journal of Visualization, Vol. 11, No. 1 (2008)95-102

Regular Paper

Experimental and Numerical Flow Visualization in a Transonic Turbine

Woisetschläger, J.*, Pecnik, R.*, Göttlich, E.*, Schennach, O.*, Marn, A.*,
Sanz, W.* and Heitmeir, F.*

* Institute for Thermal Turbomachinery and Machine Dynamics, Graz University of Technology
Inffeldgasse 25A, A – 8010 Graz, Austria. E-mail: jakob.woisetschlaeger@tugraz.at ;
URL: www.ttm.tugraz.at

Received 21 August 2007
Revised 3 November 2007

Abstract : This paper focuses on the visualization of both experimental and numerical results and presents research in a highly-loaded cold-flow transonic turbine under continuous and engine-representative conditions. Special focus was placed on blade row interaction at app. 10600 rpm. While the first step was the investigation of a single stage machine (stator-rotor), the second step extended the test rig to a one-and-a-half stage configuration (stator-rotor-stator). Measurements were carried out in the transonic test turbine at Graz University of Technology using Particle-Image-Velocimetry and Laser-Doppler-Anemometry. The main results of these experiments are discussed and compared to numerical simulations.

Keywords : Particle Image Velocimetry, turbomachinery, transonic flow, blade row interaction, computational fluid dynamics.

1. Introduction

The trend for industrial gas turbines is towards higher efficiency at constant and possibly decreasing costs per kW shaft power. Advanced 3-D aerodynamic design and higher cycle temperatures tackle the objective of higher efficiency. In order to reduce costs it is advantageous to reduce the number of stages, thus resulting in high-pressure (HP) ratios and transonic conditions for the remaining stages. Shock systems and wakes generated by stator and rotor blades cause unsteadiness in the flow through turbomachines, related to the relative motion between rotor and stator.

In multistage turbines this mixing of stator and rotor wakes from sequent stages results in a complex situation for numerical flow predictions. In subsonic flows, a number of researchers investigated these effects by measurements and numerical simulations to better understand the unsteady flow phenomena involved (Miller et al., 2003; Arnone et al., 2002). With respect to HP stages operating under transonic conditions the problem is even more complicated due to the shock waves generated by the stator and rotor blades impacting on the following cascade of blades (Jennions and Adamczyk, 1997). To find the appropriate position for the second stator row in such machines, a detailed investigation behind a transonic single-stage turbine at DLR, Germany, was performed (Tiedemann and Kost, 2001; Hummel, 2002) suggesting two axial positions behind the rotor where the shock strength is reduced and the next stator blades should be placed. This basic idea of clocking (also known as indexing) is related to the overall improvement of efficiency by varying the circumferential and/or the axial position of adjacent stator or rotor blades. Usually the

second stator is rotated with respect to the first stator (nozzle ring), with equal stator blade counts in both stators.

To investigate the unsteady but periodic flow phenomena in HP turbines and compressors a number of authors use different laser-optical techniques, e.g., Particle-Image-Velocimetry (PIV; Wernet, 2000; Lang et al., 2002; Uzol and Camci, 2002; Hayami et al., 2002; Liu et al., 2006; Göttlich et al., 2006) or Laser-Doppler-Velocimetry (LDV; Zaccaria and Lakshminarayana, 1997; Göttlich et al., 2004). These techniques avoid flow blockage and are not mechanically influenced by strong pressure fluctuations. Parallel to the recording of experimental data a number of authors developed numerical simulations for these very complex fluid flows through HP turbines (Tiedemann and Kost, 2001; Pecnik et al., 2005). Finally, a good visualization of experimental and numerical data is needed.

.

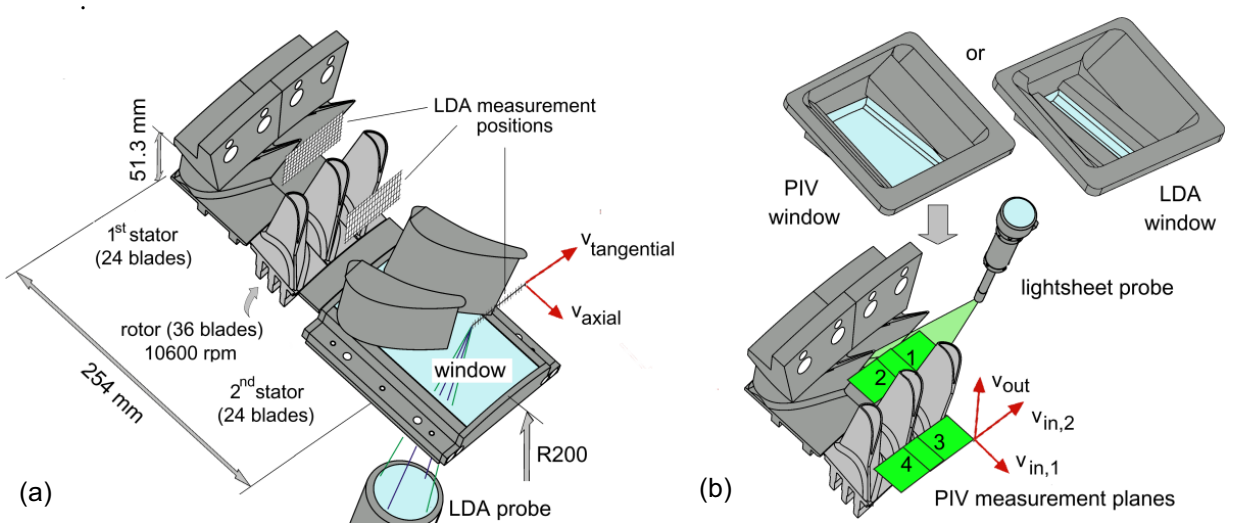

Fig. 1. Test section. (a) shows the stator-rotor-stator section of the transonic turbine with the measurement grid for Laser-Doppler-Anemometry (LDA). (b) gives the stator-rotor section with planes 1- 4 in which in-plane (in) and out-of-plane (out) components of the velocity v were recorded by Particle-Image-Velocimetry (PIV).

2. Methods Applied

2.1 Experimental Setup

The transonic test turbine of the Institute for Thermal Turbomachinery and Machine Dynamics is a continuously operating cold-flow open-circuit facility and allows the testing of turbine stages with a diameter up to 800 mm. Pressurized air is delivered to a mixing chamber by a separate 3 MW compressor station. A membrane type coupling directly transmits the turbine shaft power to a three stage radial brake compressor and measures the torque. The air temperature at turbine stage inlet can be adjusted by the compressor station coolers in a range between 40 °C to 185 °C. The maximum shaft speed of the test rig is limited to 11550 rpm.

The test section of the transonic turbine is given in Fig. 1(a). 24 stator blades are followed by 36 rotor blades and 24 stator blades in the second stator. The pressure ratio over the first stage (stator-rotor) was 3.5, the pressure ratio over all 1 ½ stages 4.27, respectively (total to static pressure ratio). Rotational speed was 10600 rpm, inlet temperature about 130-140 °C.

For the Laser-Doppler-Anemometry (LDA) optical access to the first stator - rotor section was realized through a small plane-parallel glass window (Fig. 1(b)). The Particle-Image-Velocimetry (PIV) used a plane-concave window instead (both were made of HERASIL quartz glass). Downstream the second stator a convex-concave window of 9 mm thickness and 140 × 90 mm surface dimension was used and is shown in Fig. 1(a). Anti-reflection coating was applied to all windows.

2.2 Laser Optical Measurement Techniques

For velocity recording a stereoscopic PIV (DANTEC FlowMap 1500) together with two DANTEC 80C60 HiSense cameras (1280 × 1024 pixel) and a NEW WAVE Gemini double cavity Nd:YAG laser (120 mJ/ pulse) were used. A special light-sheet optics consisting of a spherical lens (600 mm focal length), a cylindrical lens (−10 mm focal length), and a prism was used to illuminate the seeding particles in plane sections of the flow. For each camera the double images from one PIV recording were evaluated using a cross-correlation technique and an interrogation area size 64 × 64 pixel with 50 % overlap. Finally, a range validation, a correlation peak ratio validation, and a moving average validation were applied to reject invalid vectors. The time between the two pulses was 1 µs downstream of the first stator, 1.5 µs downstream the rotor. Figure 1(b) shows planes 1-4 in which the in-plane and out-of-plane components of the velocity were recorded by PIV. These components are necessary to derive the axial, circumferential and radial velocity components. Calibration was performed using a special calibration target, a 100 × 100 mm white plate with a square grid of black dots, dot spacing 2.5 mm, dot size 1.5 mm, provided by DANTEC. This target was placed in the position of the light-sheet. Finally, a map of 39 × 31 vectors was recorded for planes 1 and 2, a 39 × 29 vector map for planes 3 and 4. Planes 1 and 2 were 47.5 × 37.5 mm in size, planes 3 and 4 were 47.5 × 35 mm, respectively, all with 1.25 mm step size. See also Lang et al. 2002.

A second set of velocity data was recorded by a two-component LDA-system (DANTEC Fiber Flow with two BSA processors) using a 6W argon-ion laser (COHERENT) operated at approximately 400 mW in all lines, with the velocity component recorded in axial direction and the other component in circumferential direction (see Fig. 1(a)). The focal length used was 400 mm, the beam diameter 2.2 mm (Göttlich et al., 2006). The spacing of the measurement grid was approximately 3 mm in circumferential direction (Fig. 1(a)).

To allow analysis of the data related to the angular position of the rotor, one key-phasor reference signal and 12 TTL overspeed-tachometer signals per revolution were provided by the monitoring system of the turbine to trigger the data sampling (uncertainty: blade pitch/300, a phase delay depending on speed was accounted for). The sampling frequency by the BSA processor leads to an angular resolution of 0.01° (record interval 0,17 µs) compared to the 0.3° uncertainty caused by the trigger system. In all LDA measurement positions about 80000 velocity bursts were recorded and mapped into 40 time intervals within one blade passing period (app. 0.16 ms, corresponding to the movement of the rotor blades for one 10° section or one rotor blade pitch). Using a linear regression method presented in Glas et al., 2000, the velocities were ensemble averaged to provide velocities and turbulence levels for each of the 40 rotor-stator positions. For the PIV six angular rotor-stator positions were investigated for planes 1 to 4, using 180 sets of PIV double-images for the averaging process in each rotor stator-position. Both stators were mounted on rotatable rings. All 20 circumferential positions traversed with the LDA and the 4 planes recorded with the PIV were adjusted by moving the stators rather than moving the LDA probe or the PIV cameras.

The stator blades, the rotor blades and the endwalls were covered with a high-temperature flat black paint to reduce surface reflections. Droplets of DEHS oil (Di-Ethyl-Hexyl-Sebacin-Esther) with a nominal diameter of 0.3 µm were added by PALLAS AGF 5.0D seeding generator app. 0.3 m upstream of the first stator row as seeding material for the measurements. The fringe modulation of the burst signals was used to reduce the influence of too large droplets (BSA quality factor).

2.2 Computational Fluid Dynamics (CFD) and Data Visualization

The Computational Fluid Dynamics (CFD) was performed using the in-house Navier-Stokes code LINARS, developed at the Institute for Thermal Turbomachinery and Machine Dynamics at Graz University of Technology (Pecnik et al., 2005; Pieringer et al., 2005). The compressible Reynolds/Favre-averaged Navier-Stokes (RANS) equations in conservative form are solved by means of a fully-implicit time-marching finite-volume method on structured curvilinear grids in multiblock

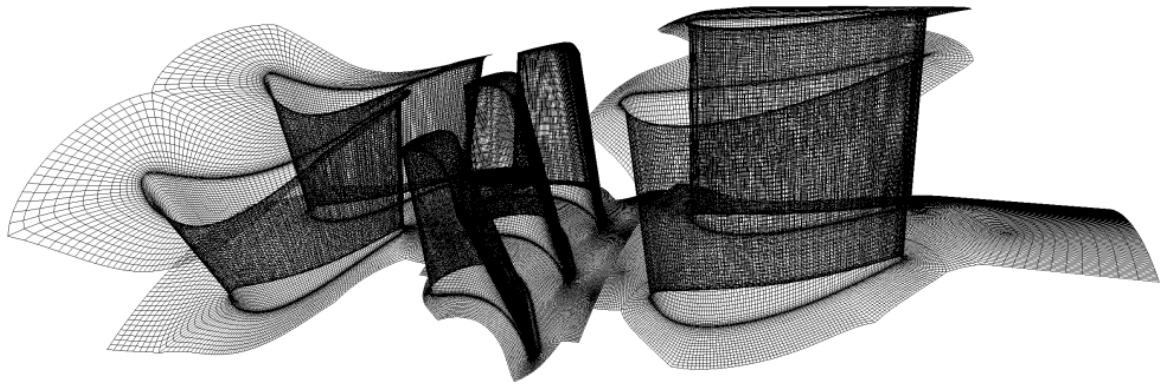

Fig. 2. Computational domain. The picture shows the surface mesh of the computational grid used for CFD. The fillets between blade and hub, blades and outer casing, as well as the rotor blade clearance are meshed to match the geometrical details of the test turbine facility. Approximately 5,000,000 cells were used for post-processing with two stator passages and three rotor passages.

alignment (see Fig. 2). To cope with unequal pitch ratios, the code uses phase-lagged boundary conditions at geometrical periodic boundaries and hence only one passage of each blade row was simulated resulting in app. 2,000,000 cells. Phase lagged boundaries are valid as long as one is not interested in large scale unsteadiness, as for any kind of other phenomena effecting the full wheel in an unsymmetrical manner. The geometrical details of the turbine stage including the fillets and the rotor tip clearance were modeled as well. These fillets were formed at the first and second stator hub, tip and the rotor hub and minimize the strains in the real machine. An O-type block encloses the blade. A thin block is arranged close to the wall faces, which covers the entire wall domain of the blades. An H-type grid block was used to model the inlet and outlet area for each blade. All together 27 blocks formed the computational domain. To save computational time and memory pressure gradient wall-functions based on the law-of-the-wall formulation by Spalding were used. The turbulence closure was done using the turbulence model of Spalart and Allmaras (Gehrer and Jericha, 1999). To achieve high order accuracy a total variation-diminishing (TVD) scheme with third-order interpolation was applied for the spatial discretization and a second order accurate Newton-Raphson procedure was applied for the integration in time. One blade passing period was calculated with 480 time steps.

Using the numerical and experimental data a final post processing is essential, since the mutual comparison facilitates understanding of the complex and unsteady flow phenomena in this type of machines. It also enables a detailed validation of numerical methods by experimental data. Thus validated by the experimental data, CFD provided new insights in the complex flow physics.

For post-processing a separate flow visualization tool was developed. This tool enables the visualization of steady as well as unsteady numerical data on structured grids. The OpenGL library was used to have access to a fast image generator to produce any desired view of the flow. It works in conjunction with a comfortable Graphical User Interface (GUI) programmed in C++. This post-processor uses a fast "marching cube" algorithm to extract iso-surfaces to draw contour plots or isolines on index surfaces ,as well as, to facilitate transparent shading of surfaces and texture mapping on surfaces with bitmaps. Further the post-processor facilitates different lightning models and the ability to define arbitrary trajectories to “fly” through datasets.

3. Results and Discussion

3.1 Stator-Rotor Interaction

First investigations using LDA, PIV and CFD techniques focused on the interaction of the first stator shock and wake system with the following rotor blades (see e.g., Göttlich et al., 2006). A flow

visualization based on all results is presented in Fig. 3, including velocity data recorded by LDA, entropy as calculated by the CFD simulation and isolines of pressure gradients (CFD) visualizing the shock system, similar to the way a Schlieren technique does. Figure 3 presents the flow phenomena within one blade passing period of approximately 0.16 ms (6360 Hz) in eight successive frames.

Within the first stator the flow accelerates to a Mach number of about 1.5, causing a pronounced shock system at the suction side of the stator blades close to the trailing edge. This shock is visible in the velocity data and by means of the pressure gradients in the CFD simulation (encircled in Fig. 3(b)). The strength and position of this shock varies slightly over the height, due to the influence of secondary flow structures close to the tip of the blade, e.g., passage vortex or tip leakage vortex. Bypassing rotor blades reflect this shock system (marked in Fig. 3(c)). In Figs. 3(d) and (h) these reflected shock waves interact with the suction side boundary layer on odd (Fig. 3(h)) and even (Fig. 3(d)) numbered stator blades due to the 2:3 ratio between stator and rotor blades. Additionally, parts of the shock waves are reflected a second time, with the second reflection at the pressure side of the rotor blades (encircled in Fig. 3(c)). This second reflection then influences the suction side boundary layer of the rotor blades.

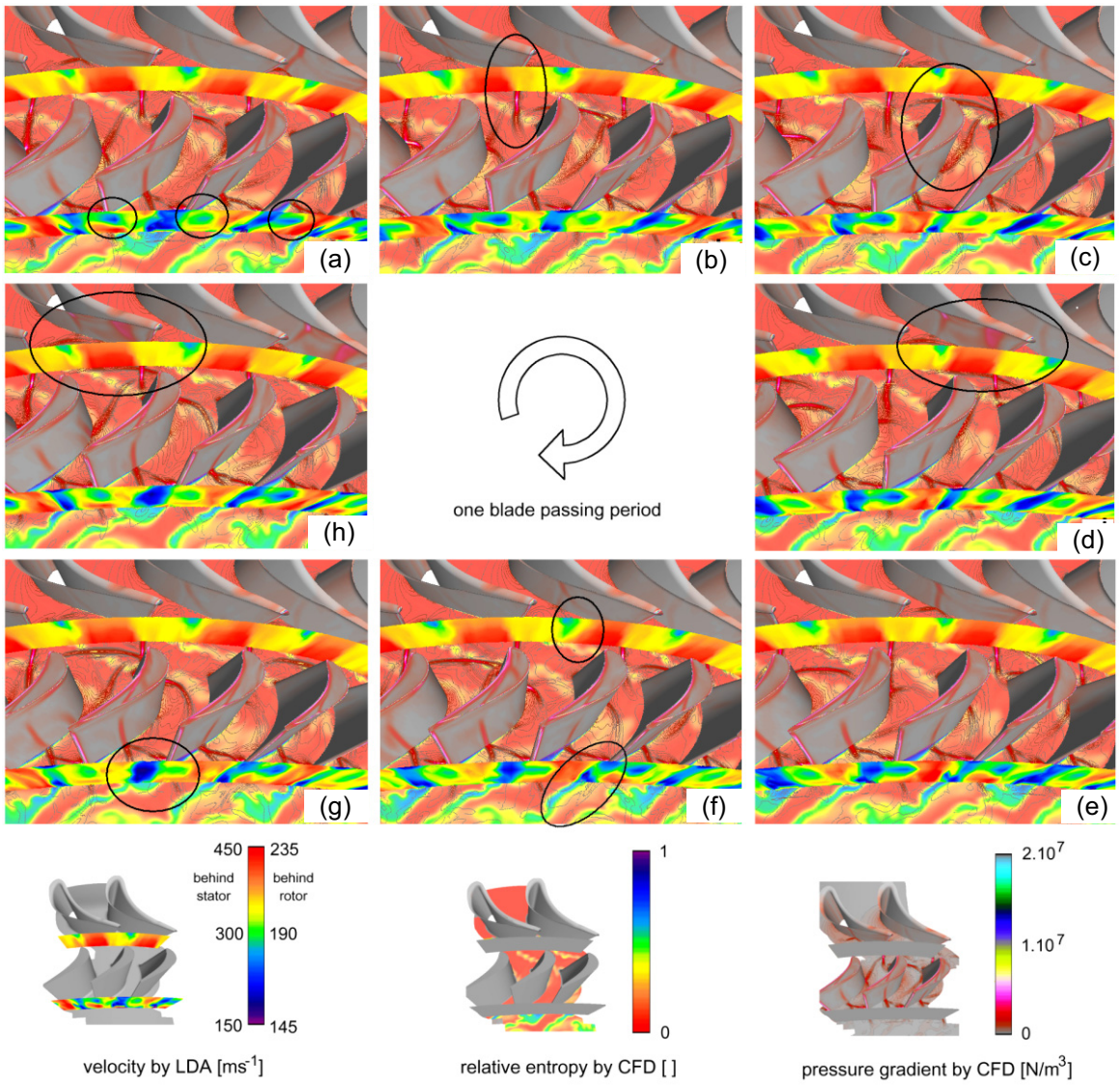

Fig. 3. Stator-Rotor interaction in a transonic turbine stage. Measurement data recorded by Laser-Doppler-Anemometry (LDA) are superimposed to the relative entropy and the pressure gradient obtained by Computational Fluid Dynamics (CFD). The eight pictures (a) – (h) present one blade passing period. Marked regions are explained in the text.

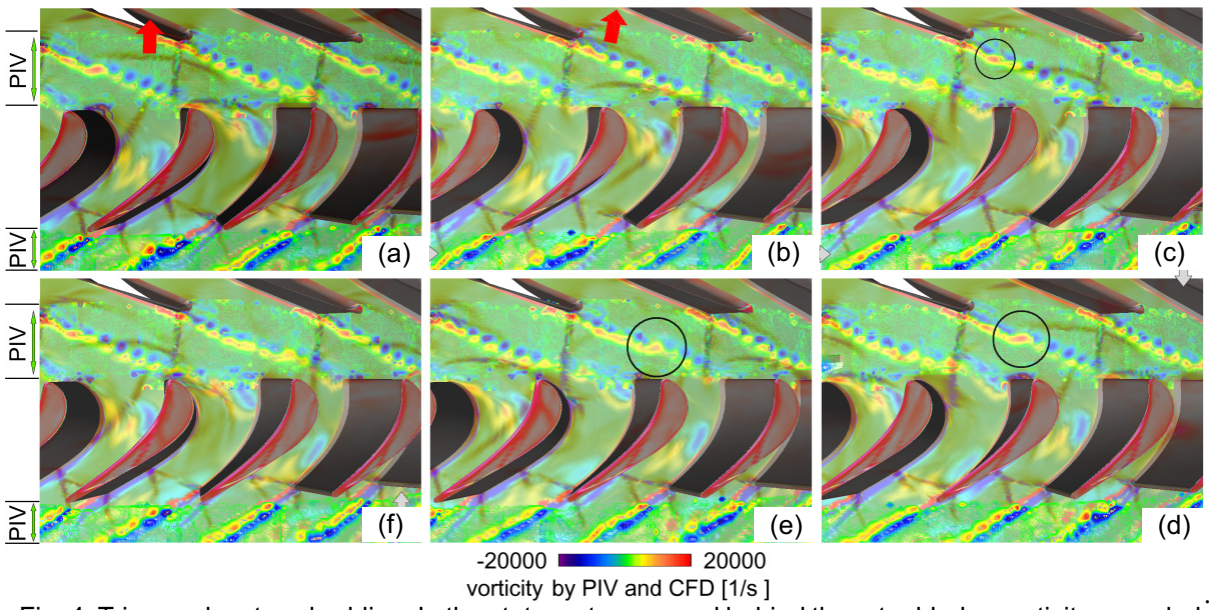

Fig. 4. Triggered vortex shedding. In the stator-rotor gap and behind the rotor blades vorticity recorded by Particle Image Velocimetry (PIV) is superimposed to results obtained by Computational Fluid Dynamics (CFD, shaded data). Regions marked by circles are explained in the text. The six frames present one blade passing period.

Behind the turbine blades shedding boundary layer material forms a vortex street, or wake. These wakes behind the stator and rotor blades are also visible in Fig. 3 in terms of relative entropy from the CFD results. Since the vortices in the wake move with lower velocity than the main flow, they are clearly visible in the velocity data obtained by LDA (circles in Fig. 3(f)). When transported through the rotor blade channel, the stator wakes are chopped by the rotor blades into single segments. These segments consist of clock-wise and counter-clock-wise rotating vortices, finally superimposed to the vortices shedding from the rotor blades. As already predicted by Hummel, 2002, vortices rotating in opposite direction increase their strength and widen the wake (marked in Fig. 3(g)). This effect and reflected shocks modulate the vortex shedding from the rotor blades. In Fig. 3(a) passage vortices behind the rotor blades are marked. These upper passage vortices, evoked by the turning of the fluid in the blade passages, migrate radially inwards due to the strong tip leakage flow (from the pressure side to suction side over the blade tip).

3.2 Triggered Vortex Shedding

All effects described in the previous chapter can also be studied in Fig. 4 in terms of vorticity recorded by PIV and calculated by CFD. In this figure the PIV data are presented as isolines in the sections marked, superimposed to the results obtained by CFD (shaded). Additionally, the shock waves are visualized by brownish contours of pressure gradient (CFD).

In Fig. 4(a) a shock wave reflected by two bypassing rotor blades is marked by a red arrow. At 10600 rpm this reflection move towards the suction side of the stator blades. When this shock wave hits the suction side of the stator blade in Fig. 4(b), the boundary layer shedding at the trailing edge is first disrupted and then shedding of a very pronounced vortex is enforced. This vortex is marked in Figs. 4(c), (d) and (e). Half a blade passing period later vortex shedding from this stator blade is back to normal (Fig. 4(f)). Due to this interaction between the shock waves and the boundary layer, the vortex shedding is in phase with the bypassing rotor blades.

3.3 Clocking of Stator Blades

The information discussed in the previous sections is of relevance to the engineer when clocking is concerned. Figure 5 presents two different angular positions for the second stator row relative to the

first stator row (clocking positions "(a)" and "(b)"). Detailed measurements of 10 different clocking positions indicated that for the mid-section flow clocking results in a ±1.6 % variation in efficiency, with an efficiency maximum in position (b) in Fig. 5 and a minimum in position "(a)".

The rotor blades chop the wake from the first stator and by the wake-wake interaction between the first stator wake and the rotor wake large vortices are produced (indicated by circles in Fig. 5). These vortices can be identified by their higher turbulent kinetic energy and entropy. In clocking position "(a)", these vortices move through the channel of the second stator and cause strong variations in turbulent kinetic energy and flow angle, negatively affecting efficiency. On the right side of Fig. 5, the turbulent kinetic energy recorded by LDA is presented as time-space plot. In this plot time is given in terms of blade passing period along the abscissa and space in terms of measurement positions along the ordinate (two blade pitches). In such a 2:3 diagram the two stator wakes show up as horizontal structures, while the influence from the rotor blades is 45° inclined.

In Fig. 5 position (b) the chopped wake of the first stator blade passes the second stator blade close to its pressure side, with minimum influence on the suction side boundary layer. Additionally, the impingement of shock waves from the rotor exit at the second stator is less pronounced in position (b). This is due to the fact that the shock system forming at the rotor blade exit is also modulated by the bypassing first stator wakes (see Figs. 4(a)-(f)) and the axial distance between rotor and second stator meets the needs (for more details see also Schennach et al., 2007; Additional images from this stage can be found in Woisetschläger et al., 2007).

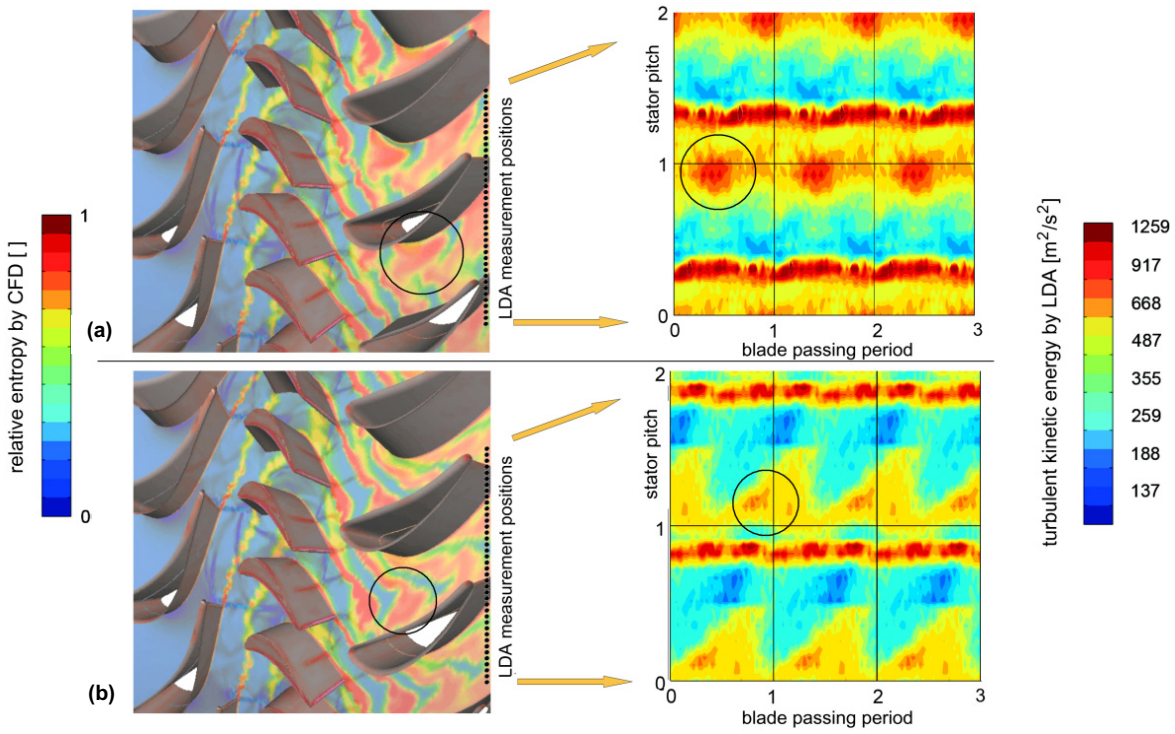

Fig. 5. The clocking of stator blades (positions (a) and (b)) is discussed by means of the relative entropy calculated by Computational Fluid Dynamics (CFD) and the turbulent kinetic energy recorded by Laser-Doppler-Anemometry (LDA).

4. Conclusion

Operating under transonic conditions, high-pressure turbines show complex flow physics mainly due to the shock systems generated by stator and rotor blades. These shocks have a strong tendency to trigger certain flow phenomena, e.g., vortex shedding from the trailing edges of the turbine blades. Superimposed in phase these effects might add up over the single stages. Proper positioning of the

second stator blades will decrease the strength of this interference. Additionally, secondary flow phenomena like passage vortices and tip vortices alter these phenomena over the blade height, therefore a full three-dimensional flow design is essential. Visualization of numerical and experimental data is a powerful tool to facilitate validation during post-processing

Acknowledgements

This work was made possible by the Austrian Science Fund (FWF) within the grants P16521-N07 "Experimental Investigation of the Stator-Rotor-Stator Interaction in a Transonic Turbine", Y57-TEC "Non-intrusive Measurement of Turbulence in Turbomachinery" and P16761 "Steady and Unsteady Transition Modelling". The support of Dr. H. P. Pirker in the operation of the compressor station is also gratefully acknowledged. Graz University of Technology is member of the thematic network "PIV-NET 2" funded by the European Union.

References

Arnone, A., Marconcini, M., Pacciani, R., Schipani, C. and Spano, E., Numerical investigation of airfoil clocking in a three-stage low-pressure turbine, ASME J Turbomachinery, 124 (2002), 61-68.

Glas, W., Forstner, M., Kuhn, K. and Jaberg, H., Smoothing and statistical evaluation of Laser-Doppler-Velocimetry data of turbulent flows in rotating and reciprocating machinery, Exp. Fluids, 29 (2000), 411-417.

Göttlich, E., Neumayer, F., Woisetschläger, J., Sanz, W. and Heitmeir, F., Investigation of stator-rotor interaction in a transonic turbine stage using Laser Doppler Velocimetry and pneumatic probes, ASME J Turbomachinery, 126 (2004), 297-305.

Göttlich, E., Woisetschläger, J., Pieringer, P., Hampel, B. and Heitmeir, F., Investigation of vortex shedding and wake-wake interaction in a transonic turbine stage using Laser-Velocimetry and Particle-Image-velocimetry, ASME J Turbomachinery, 128 (2006), 178-187.

Hayami, H., Hojo, M. and Aramaki, S., Flow measurement in a transonic centrifugal impeller using a PIV, Journal of Visualization, 5-3 (2002) 255-262.

Hummel, F., Wake-wake interaction and its potential for clocking in a transonic high-pressure turbine, ASME J Turbomachinery, 124 (2002), 69-76.

Jennions, I. K. and Adamczyk, J. J., Evaluation of the interaction losses in a transonic turbine HP rotor / LP vane Configuration, ASME J Turbomachinery, 119 (1997), 69-76.

Lang, H., Mørck, T. and Woisetschläger, J., Stereoscopic particle image velocimetry in a transonic turbine, Exp.Fluids, 32 (2002), 700-709.

Liu, B., Yu, X., Liu, H., Jiang, H., Yuan, H. and Xu, Y., Application of SPIV in turbomachinery, Exp. Fluids, 40 (2006), 621-642.

Miller, R.J., Moss, R.W., Ainsworth, R. W. and Horwood, C.K., Time-resolved vane-rotor interaction in a high-pressure turbine stage, ASME J. Turbomachinery, 125 (2003), 1-13.

Pecnik, R., Pieringer, P. and Sanz, W., Numerical investigation of the secondary flow through a transonic turbine stage using various turbulence closures, Proceedings of the ASME TURBO EXPO 2005, (Reno, USA), paper GT2005-68754, (2005).

Gehrer, A. and Jericha, H., External Heat Transfer Predictions in a Highly-Loaded Transonic Linear Turbine Guide Vane Cascade using an Upwind Biased Navier-Stokes Solver, ASME J Turbomachinery, 121(1999), 525-531.

Pieringer, P., Göttlich, E., Woisetschläger, J., Sanz, W. and Heitmeir, F., Numerical Investigation of the Unsteady Flow through a Transonic Turbine Stage Using an Innovative Flow Solver, Proceedings 6th European Conference on Turbomachinery, (Lille, France), (2005), 339-352.

Schennach. O., Woisetschläger, J., Fuchs, A., Göttlich, E., Marn, A. and Pecnik, R., Experimental Investigations of Clocking in a 1 ½ Stage Transonic Turbine using Laser-Doppler Velocimetry and a Fast Response Aerodynamics Pressure Probe, ASME J Turbomachinery, 129 (2007), 372-381.

Tiedemann, M. and Kost, F., Some aspects of wake-wake interactions regarding turbine stator clocking, ASME J Turbomachinery, 123 (2001), 526-533.

Uzol, O. and Camci, C., Experimental and computational visualization and frequency measurements of the jet oscillation inside a fluidic oscillator , Journal of Visualization, 5-3 (2002),263-273.

Wernet ,M. P., Development of digital particle image velocimetry for use in turbomachinery, Exp Fluids, 28 (2000), 97-115.

Woisetschläger, J., Pecnik, R., Göttlich, E., Schennach, O., Marn, A., Sanz, W. and Heitmeir, F., Laser-Optical Investigation of Stator-Rotor Interaction in a Transonic Turbine, Journal of Visualization, 10-1 (2007), 6.

Zaccaria, M. A. and Lakshminarayana, Unsteady flow field due to nozzle wake interaction with the rotor in a axial flow turbine: part 1 – rotor passage flow field, ASME J Turbomachinery, 119 (1997), 201-213.

Author Profile

Jakob Woisetschläger: He received his M.Sc. (Dipl.-Ing.) in 1987 and his Ph.D. in Physics in 1990 from Graz University of Technology with distinction. Exchange student in 1986 at the Institute for Physics, University of Zagreb, Croatia. 1991-1992 Visiting Scientist at the Institute for Biomedical Engineering Research, University of Akron, Ohio USA. Since 1998 Associate Professor at Graz University of Technology. Since 2002 head of the work-group "Experimental Turbomachinery research and Optical Diagnostics" at the Institute for Thermal Turbomachinery and Machine Dynamics, Graz University of Technology. In 2004 and 2005 visiting exchange program with RWTH Aachen, Germany and University Zaragoza, Spain. In 1996 Young Scientist START Award granted by the Austrian Chancellor, in 2004 Research Award granted by the Governor of Styria. Author (co-author) of more than 100 contributions to books, journals and conference proceedings, Author (co-author) of about 30 reports and application notes, one patent. Member International Society for Optical Engineering SPIE and Austrian Physical Society OEPG.